Three-Way Outlier Detection Based on Shadowed Granular-Balls

Jie Yang, Feng Lu, Guoyin Wang, *Senior Member, IEEE*, Shuyin Xia, Qinghua Zhang, *Senior Member, IEEE*, Yi Liu, Yi Wang, Di Wu

***Abstract*—Most existing outlier detection methods rely on a single and fine-grained data representation, making them vulnerable to noise and inefficient in capturing local anomalies. Granular-ball computing (GBC), as an emerging multi-granularity representation and computation framework, provides an effective means to address these issues. Meanwhile, shadow set theory offers a flexible mechanism using three-way decision to handle uncertainty and boundary fuzziness in data. The integration of GBC with shadow set theory combines the strengths of both frameworks, offering promising potential for outlier detection tasks. In this study, we propose a novel outlier detection based on shadowed granular-balls. Firstly, we propose an unsupervised granular-ball generation method with the principle of justifiable granularity. Then, we further present an outlier detection method, named three-way outlier detection based on shadowed granular-ball (3W-SGBD). 3W-SGBD introduces an unsupervised granular-ball generation strategy guided by local density clustering, and adaptively splits granular-balls through a dual-entropy-driven mechanism to better capture local anomalies. In addition, by partitioning each granular-ball into positive, negative, and boundary regions via shadow mapping, 3W-SGBD refines boundary areas to enhance detection accuracy. Finally, extensive comparative experiments are conducted with several state-of-the-art baseline methods on 16 public benchmark datasets. The results show that the effectiveness, efficiency, and robustness of the method proposed in this paper. The code is publicly available at https://github.com/2257352568/3W-SGBD.**

***Index Terms*—Granular-ball computing, Shadowed granular-balls, Three-way decision, Justifiable granularity, Outlier detection**

I. Introduction

OUTLIER detection [1] is a fundamental research area in machine learning and data mining, aiming to identify data points that deviate significantly from normal patterns. It plays a crucial role in various applications such as fraud detection [2], network security [3], and industrial fault diagnosis [4]. Therefore, the study of outlier detection methods has significant research and practical value. However, existing outlier detection methods still face challenges when dealing with high-dimensional, noisy, and complex data distributions.

Current outlier detection methods can be broadly classified into statistical-based [5], distance-based [6], density-based [7], clustering-based [8], and rough set theory-based approaches [9]. Each exhibits distinct advantages and limitations in different application scenarios. Statistical-based methods heavily rely on prior distributional assumptions, making them less effective when dealing with complex, multimodal, or unknown data distributions. Their performance is particularly limited in real-world scenarios where the data distributions are highly dynamic and difficult to model explicitly. Although distance-based methods are intuitive and effective for low-dimensional data, they suffer from the curse of dimensionality, which causes distance metrics to lose discriminative power as data dimensionality increases. Additionally, distance-based methods [10] are highly sensitive to parameter selection, particularly the choice of neighborhood size. However, the performance of clustering-based methods heavily depends on parameter selection, and they often struggle with datasets exhibiting non-convex distributions, reducing their effectiveness in detecting complex anomalies. Rough set theory-based methods [11] emphasize multi-granularity analysis of data, leveraging granular computing principles to extract anomalous features across different granularity levels. These approaches construct lower and upper approximation boundaries to model uncertainty within the data, making them particularly suitable for outlier detection in incomplete or imprecise data environments.

Density-based methods [12] identify anomalies by analyzing variations in local density, under the assumption that anomalies are typically located in low-density regions. One of the most well-known methods in this domain is the local outlier factor (LOF), which quantifies the outlier degree of a point by comparing its local density to that of its neighbors. This concept has been extended with algorithms such as the connectivity-based outlier factor (COF) [13] and the influenced outlierness (INFLO) [14], which incorporate connectivity patterns and multi-directional density estimates to improve the precision of outlier detection. To mitigate the challenges of fixed neighborhood sizes and improve flexibility, Campello [15] introduced the HDBSCAN algorithm, which performs hierarchical density-based clustering by automatically adapting to variations in data density. This approach identifies anomalies as points outside the persistent clusters formed during the hierarchical process. Although the traditional outlier detection methods have demonstrated effectiveness under spe-

✉ Corresponding author: Di Wu. Di Wu is with the College of Computer and Information Science, Southwest University, Chongqing 400715, China. (E-mail: wudi.cigit@gmail.com).

Jie Yang is with the Key Laboratory of Cyberspace Big Data Intelligent Security, Ministry of Education, Chongqing University of Posts and Telecommunications, Chongqing 400065, China, with the School of Physics and Electronic Science, Zunyi Normal University, Zunyi 563002, China. (E-mail: yj530966074@foxmail.com).

Guoyin Wang is with the National Center for Applied Mathematics in Chongqing, Chongqing Normal University, Chongqing 401331, China. (E-mail: wanggy@cqnu.edu.cn).

Feng Lu, Qinghua Zhang and Shuyin Xia are with the School of Computer Science and Technology, Chongqing University of Posts and Telecommunications, Chongqing 400065, China. (E-mail: luf.cqupt@gmail.com, zhangqh@cqupt.edu.cn, xiasy@cqupt.edu.cn).

cific conditions, they face significant challenges when applied to high-dimensional, noisy, and complex data distributions. Key limitations include sensitivity to local data structures, high computational complexity, dependency on parameter tuning, and inadequate granularity in outlier classification. Therefore, developing efficient, robust, and interpretable outlier detection methods remains an important research direction in the field.

In recent years, granular computing (GrC) [16], [17] has emerged as a promising paradigm for solving complex problems. Based on the idea of GrC, granular-ball computing (GBC), introduced by Xia [18], [19], has demonstrated notable advantages in noise robustness and computational efficiency through the adaptive generation of multi-scale granular-balls (GBs). Unlike conventional point-based representations, GBC constructs GBs by grouping multiple data points, thereby shifting the learning process from an individual sample-level perspective to a coarse-grained approach. As a result, GBC significantly enhances processing efficiency without compromising essential data structures. Currently, many scholars have proposed different improvements. Qian [20] explored the application of GBC in multi-label classification tasks and proposed a framework that combines GBC with multi-label learning to effectively improve classification accuracy. Yang [21] presented serveral GB-based classifiers from the perspective of three-way decision. Xie [22] proposes a multi-granularity neighbor relationship framework using GBC to enhance both efficiency and accuracy of KNN and clustering methods.

Recently, multi-granularity characteristic and robustness of GB make it excellent in multiple applications, especially in outlier detection. Bai [23] introduced an outlier detection method based on GB clustering, where anomalies were identified by analyzing internal sample count, overlapping relations, and domain variations within each GB. Su [24] proposed an outlier detection framework leveraging granular-ball fuzzy rough sets (GBFRD) based on the fuzzy approximation accuracy. More recently, Cheng [25] proposed a granular-ball mean-shift outlier detector (GBMOD) integrated GBC with the mean-shift algorithm to estimate shifted centers. Although these methods improve outlier detection performance over traditional point-based techniques, they generally rely on hard assignments of samples to granular-balls, overlooking the ambiguity at GB boundaries. In addition, they often lack mechanisms for modeling data uncertainty, which may result in a decline in the accuracy of outlier detection.

As is well known, three-way decision (3WD) theory [26], [27] proposed by Yao has emerged as a promising approach to tackle complex problems involving uncertainty. The fundamental principle of 3WD lies in dividing a universe into three distinct regions, with each region corresponding to a specific decision action. As a generalization of the traditional two-way decision model, 3WD further incorporates a third option, enabling a trisecting-and-acting approach to decision-making. This approach not only enhances robustness against ambiguous or noisy data but also improves decision interpretability by clearly identifying cases that require further analysis. Based on the above discussion, we propose an innovative three-way outlier detection based on shadowed granular-balls (3W-SGBD), which integrates GBC with 3WD theory to enhance outlier detection in uncertain environments.

The framework diagram of 3W-SGBD is shown in Fig. 1. First, the shadowed granular-balls are generated using a recursive splitting mechanism driven by a composite loss function that integrates coverage entropy and specificity entropy. Then, based on the fuzzy membership degrees, each sample is assigned to positive, negative, or boundary regions across the GBs according to three-way decision strategy. The outlier score of each object is calculated by fusing its regional information across multiple GBs. Finally, the outlier factors are compared with a threshold ξ to identify the anomalies and accomplish outlier detection. Specifically, the contributions of this study include:

(1) Combine with dual-entropy-driven, we propose an improved GB generation method with the principle of justifiable granularity.
(2) We introduce 3WD to construct and optimize shadowed GBs for modeling uncertain data.
(3) Based on our proposed membership-based factor with shadowed GBs, this paper propose a three-way outlier detection based on shadowed granular-balls (3W-SGBD).

The remainder of this study is organized as follows. Section II introduces the preliminary knowledge on shadowed sets, GBC and three-way decision. In Section III, an improved GB generation method is constructed based on the principle of justifiable granularity. Section IV presents the construction of shadowed granular-balls and details the 3W-SGBD algorithm and outlier factor calculation. The results of our experiments are shown in Section V. Finally, Section VI summarizes this study and discusses future research directions.

II. Preliminaries

In this section, to set up the framework of this paper, we recall some necessary definitions related to shadowed sets, GB and 3WD.

Definition 1. [28] Let the information system (IS) be a 4-tuple $IS = \langle U, A, V, f \rangle$, where $U = \{x_1, x_2, \ldots, x_n\}$ denotes a non-empty finite set of objects; A is the non-empty finite set of attributes; $V = \bigcup_{a \in A} V_a$ is the union of domain V_a of attribute a, and $f : U \times A \to V$ denotes an information function that maps an object in U.

Shadowed sets [29] was proposed by Pedrycz and constructed through the fuzzy-rough transformation of fuzzy sets. This provided an effective tool to model and analyze the concepts with uncertainty. We can describe fuzzy-rough transformation as follows:

Definition 2. [30] Let $U = \{x_1, x_2, \ldots, x_n\}$ be a non-empty finite set. A fuzzy set $\widetilde{A}$ in U is characterized by a membership function $\mu_{\widetilde{A}} : U \to [0, 1]$. For each element $x \in U$, $\mu_{\widetilde{A}}(x)$ denotes the membership degree of x to the fuzzy set $\widetilde{A}$.

Definition 3. [29] Let $U = \{x_1, x_2, \ldots, x_n\}$ be a non-empty finite set. For each sample $x \in U$, $\mu_{\widetilde{A}}(x)$ denotes the fuzzy membership of x in fuzzy set $\widetilde{A}$. The process of mapping these memberships into a triplet set $\{0, [0, 1], 1\}$ is called

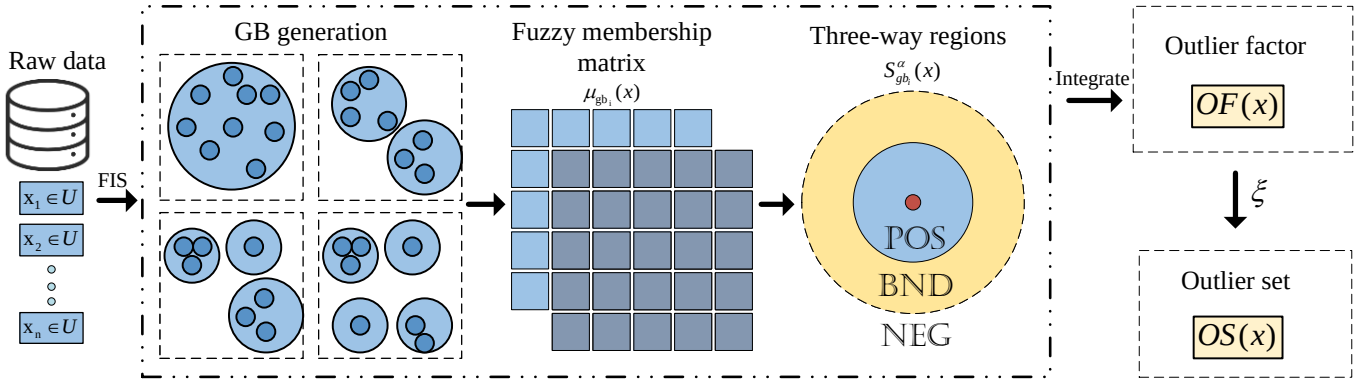

Fig. 1: The framework diagram of 3W-SGBD.

fuzzy-rough transformation, and the mapping is formulated as follows:

$$S^{\alpha,\beta}_{\mu_{\widetilde{A}}}(x) = \begin{cases} 1, & \mu_{\widetilde{A}}(x) \geq \beta \\ [0,1], & \alpha < \mu_{\widetilde{A}}(x) < \beta \\ 0, & \mu_{\widetilde{A}}(x) \leq \alpha \end{cases} \tag{1}$$

where $0 \leq \alpha < \beta \leq 1$ are the threshold parameter, and after that mapping, we get a shadowed set by threshold pair (α, β).

During this transformation, membership values less than α are assigned to 0, while those greater than β are mapped to 1. This process inevitably results in a loss of membership information, referred to as uncertainty variance. The uncertainty variance arising from converting fuzzy memberships into a shadowed set can be formulated as follows:

Definition 4. [31] Let $U = \{x_1, x_2, \ldots, x_n\}$ be a non-empty finite set. For each sample $x \in U$, $\mu_{\widetilde{A}}(x)$ denotes the fuzzy membership of x in fuzzy set $\widetilde{A}$, and $S^{\alpha,\beta}_{\mu_{\widetilde{A}}}(x)$ is a fuzzy-rough transformation on $\widetilde{A}$. The uncertainty variance $V(\alpha, \beta)$ of this fuzzy-rough transformation is formulated as:

$$\begin{aligned} V(\alpha,\beta) &= \sum_{x\in U} \left| \mu_{\widetilde{A}}(x) - S^{\alpha,\beta}_{\mu_{\widetilde{A}}}(x) \right| \\ &= \Bigg| \sum_{\mu_{\widetilde{A}}(x)\leq\alpha} S^{\alpha,\beta}_{\mu_{\widetilde{A}}}(x) + \sum_{\mu_{\widetilde{A}}(x)\geq\beta} (1 - S^{\alpha,\beta}_{\mu_{\widetilde{A}}}(x)) \\ &\quad - card\{x|\alpha < \mu_{\widetilde{A}}(x) \leq \beta\} \Bigg| \end{aligned} \tag{2}$$

To quantify the uncertainty within a fuzzy set, Zhang [32] introduced the concept of average fuzziness, which can be defined as follows:

Definition 5. [32] Let $U = \{x_1, x_2, \ldots, x_n\}$ be a non-empty finite set. For each sample $x \in U$, $\mu_{\widetilde{A}}(x)$ denotes the fuzzy membership of x in fuzzy set $\widetilde{A}$, the fuzziness of x is defined as:

$$\hbar(x) = 4\mu_{\widetilde{A}}(x)(1 - \mu_{\widetilde{A}}(x)) \tag{3}$$

The average fuzziness of U is represented by:

$$\Gamma(U) = \frac{1}{|U|} \sum_{x\in U} \hbar(x) \tag{4}$$

The three-way decision (3WD) model [33] extends the traditional binary decision framework by introducing a third option. Instead of making a strict binary choice, 3WD divides the universe into three distinct regions: positive region (acceptance), negative region (rejection), and boundary region (noncommitment). This provides a more flexible decision-making structure when uncertainty is present. The application of 3WD to a fuzzy set can be formulated as follows:

Definition 6. [33] Let $U = \{x_1, x_2, \ldots, x_n\}$ be a non-empty finite set. For each sample $x \in U$, $\mu_{\widetilde{A}}(x)$ denotes the fuzzy membership of x in fuzzy set $\widetilde{A}$. Given two thresholds α and β $(0 \leq \alpha < \beta \leq 1)$, 3WD divides the three regions based on $\mu_{\widetilde{A}}(x)$ are defined as:

$$\begin{aligned} POS_{\alpha,\beta} &= \{x \in U | \mu_{\widetilde{A}}(x) \geq \beta\} \\ NEG_{\alpha,\beta} &= \{x \in U | \mu_{\widetilde{A}}(x) \leq \alpha\} \\ BND_{\alpha,\beta} &= \{x \in U | \alpha < \mu_{\widetilde{A}}(x) < \beta\} \end{aligned} \tag{5}$$

GBC [18] is a robust and efficient GrC method. Unlike traditional approaches that focus solely on the finest granularity of individual sample points, GBC introduces GBs to replace single-granularity sample points, enabling a multi-granularity representation of data.

Definition 7. [18] Let $U = \{x_1, x_2, \ldots, x_n\}$ be a non-empty finite set, and $G = \{gb_1, gb_2, \ldots, gb_m\}$ is a granular-ball space of U. For each $gb_i \in G$, $gb_i = \{x_{i1}, x_{i2}, \ldots, x_{i|gb_i|}\}(i = 1, 2, \ldots, m)$, its attributes can be defined as follows:

$$\begin{aligned} c_{gb_i} &= \frac{1}{|gb_i|} \sum_{j=1}^{|gb_i|} x_{ij}, \qquad r_{gb_i} = \frac{1}{\lambda|gb_i|} \sum_{j=1}^{|gb_i|} \|x_{ij} - c_{gb_i}\|, \\ l_{gb_i} &= \arg\max_{l_k} |\{x_{ij} | l_{ij} = l_k\}|, \quad p_{gb_i} = \frac{|\{x_{ij} \mid l_{ij} = l_{gb_i}\}|}{|gb_i|} \end{aligned} \tag{6}$$

where c_{gb_i} is the center, r_{gb_i} is the radius, λ is a radius scaling factor that helps avoid the interference of extreme radii on outlier detection, l_{gb_i} is the label, and p_{gb_i} is the purity of gb_i. $l_{ij}(j = 1, 2, ..., |gb_i|)$ is the label of x_{ij}, $l_k(k = 1, 2, ..., z)$ represents different labels in gb_i.

Based on the definition, the center of GB is computed as the center of gravity of all objects within it, and its radius is the average distance from these objects to the center. Alternatively, the radius can be defined using the maximum distance among the objects, which enables the GB to encompass the original data more completely. In practice, the average distance is commonly used in classification tasks because it produces clear decision boundaries, while the maximum distance is favored in clustering tasks to ensure comprehensive data coverage.

In traditional GB-based classification tasks, the quality of GB is often assessed using purity, which measures the proportion of samples from the majority class within GB. However, such label-dependent evaluation is unsuitable for unsupervised outlier detection, as label information is not available. Consequently, in this study, we adopt a label-independent GB generation strategy. The details will be introduced in the following sections. As a preparation, the main symbolic variables of this paper are shown in Table I.

TABLE I: Main symbolic variables of this paper.

Symbol	Description
c_i	Center of the i-th granular-ball.
r_i	Radius of the i-th granular-ball.
λ	Radius scaling parameter, adjusting the average deviation to determine granular-ball radius.
$\mu_{gb_i}(x)$	Membership degree of sample x to granular-ball gb_i.
σ	Membership sensitivity parameter, controlling the fuzziness of membership degree.
$\mathbb{E}^c_{gb_i}$	Coverage entropy of gb_i.
$\mathbb{E}^s_{gb_i}$	Specificity entropy of gb_i.
θ	Entropy weight parameter, balancing coverage entropy and specificity entropy.
α, β	Adaptive thresholds derived from the membership distribution.
$OF(x)$	Outlier factor of sample x.

III. Dual-entropy-driven granular-ball generation method

The quality of GB plays a crucial role in the GB generation process. During this process, it is essential to evaluate the quality of each GB to determine whether further division is necessary. The generation process continues until all GB satisfy the predefined quality criteria. The quality of GB has a significant impact on the performance of downstream tasks. In traditional settings of GB generation, GB quality is typically defined based on the class labels of the objects within each GB, particularly in classification tasks. In recent years, several unsupervised GB generation strategies have been proposed to handle unlabeled data [34], [35]. However, they often rely on a single structural criterion, such as maximizing density concentration or minimizing radius [36]–[38]. As a result, the generated GBs may become overly large, which obscures subtle anomalies, or too small, which leads to the loss of important information. These limitations hinder their ability to effectively capture anomalies within complex data distributions and reduce their robustness in identifying outliers embedded in dense or overlapping regions.

In this study, we propose a label-free GB generation strategy based on combined entropy from the perspective of justifiable granularity [34], [39]. Instead of using label-based purity, a composite loss function is employed to guide the recursive division of GBs. This loss function integrates two components: coverage entropy and specificity entropy [40]. This strategy encourages GBs to represent sufficient data mass and evaluates the density concentration within each GB, respectively. This ensures that each split simultaneously improves data representation while preserving local density information. For clarity, the original granular-ball generation procedure is provided in Section S1 of the supplementary file.

Definition 8. Let $U = \{x_1, x_2, \ldots, x_n\}$ be a non-empty finite set, and $G = \{gb_1, gb_2, \ldots, gb_m\}$ is a granular-ball space of U. For each $gb_i \in G (i = 1, 2, \ldots, m)$, the coverage entropy of gb_i is formulated as follows:

$$\mathbb{E}^c_{gb_i} = -\frac{|gb_i|}{|U|} \log \frac{|gb_i|}{|U|} \tag{7}$$

The specificity entropy of gb_i is formulated as follows:

$$\mathbb{E}^s_{gb_i} = -\sum_{x_j \in gb_i} p_j \log p_j \tag{8}$$

where $p_j = \frac{\rho_j}{\sum_{x_j \in gb_i} \rho_j}$ denotes the local normalized density of sample x_j within gb_i, and $\rho_j = \exp[-(\frac{x_j - c_{gb_i}}{r_{gb_i}})^2]$ measures the local density of x_j based on its distance to the center of gb_i.

Coverage entropy refers to a GB that covers as much experimental data as possible. From the properties of information entropy, it is easy to deduce that coverage entropy strictly increases with the split of GBs. That is, when there is only an initial GB, coverage entropy takes the minimum value of 0, and when all GBs are split into single sample, coverage entropy takes the maximum value. Specificity entropy captures the density structure of the samples within a GB. Similar to coverage entropy, specificity entropy takes the maximum value when there is only an initial GB, and takes the minimum value of 0 when all GBs are split into single sample. Specificity entropy decreases with the split of GB. The detailed proof for the monotonicity of coverage entropy and specificity entropy with the granularity being finer can be found in Section S2 of the supplementary file. Therefore, coverage entropy and specificity entropy are contradictory. To balance these two entropies and achieve the justifiable granularity in the GB generation, we define the composite loss function as a weighted combination of coverage entropy and specificity entropy. This facilitates the generation of GBs that are both informative and structurally meaningful. The loss function is defined as follows:

$$\mathbb{L}_G = \theta \mathbb{E}^c_G + \varepsilon(1-\theta)\mathbb{E}^s_G \tag{9}$$

where $\mathbb{E}^c_G = \sum_{gb_i \in G} \mathbb{E}^c_{gb_i}$ and $\mathbb{E}^s_G = \sum_{gb_i \in G} \mathbb{E}^s_{gb_i}$. θ is a parameter that controls the weight of two entropies and $\varepsilon = \frac{\max \mathbb{E}^c_G}{\max \mathbb{E}^s_G}$ is an adaptive parameter that balances the

Algorithm 1: Dual-entropy-driven granular-ball generation.

Input: Datasets D, entropy weight parameter θ, radius scaling factor λ, granular-ball size $min\_samples$;
Output: Granular-ball space G;
Initialize granular-ball $gb \leftarrow D$;
Initialize priority queue $Q \leftarrow \varnothing$, granular-ball set $G \leftarrow \varnothing$;
Calculate $\mathbb{L}_{gb}$, push gb into Q in descending order of $\mathbb{L}_{gb}$;
while $Q \neq \varnothing$ **do**
  Pop granular-ball gb from Q;
  if $|gb| <$ *min_samples* **then**
    $G \leftarrow G \cup \{gb\}$;
  else
    split gb into gb_i by HDBSCAN ;
    Initialize sub-ball set $S \leftarrow \varnothing$;
    for each gb_i **do**
      $S \leftarrow S \cup \{gb_i\}$;
    end
    Calculate $\mathbb{L}'_{gb} \leftarrow \sum \mathbb{L}_{gb_i}, \forall gb_i \in S$;
    if $\mathbb{L}'_{gb} < \mathbb{L}_{gb}$ **then**
      Push all $gb_i \in S$ into Q in descending order of $\mathbb{L}_{gb}$;
    else
      $G \leftarrow G \cup \{gb\}$;
    end
  end
end
return G.

slope of two entropies. This loss function encourages the generation of GBs that maintain broad data coverage while preserving local structural compactness. Only the splits that reduce the overall loss are accepted, ensuring meaningful and interpretable granular refinement.

Algorithm 1 shows our proposed dual-entropy-driven GB generation. The GB generation is formulated as a recursive splitting process driven by a composite loss function, which integrates coverage entropy and specificity entropy. HDBSCAN automatically determines the number and shape of clusters based on a hierarchical density structure, reducing sensitivity to hyperparameter tuning. And It adaptively extracts clusters of varying densities while marking noise explicitly, which is essential for modeling fine-grained local anomalies. Building upon these strengths, we employ it as the clustering mechanism to divide each GB based on local density structures. Algorithm 1 introduces an unsupervised evaluation strategy, that is, a GB is retained if it cannot be further split into child GBs that reduce the total loss. The entire process follows a greedy optimization paradigm using a priority queue, in which GBs with higher loss are given higher priority for splitting. Given that clusters are extracted efficiently and each split is evaluated only when necessary, the practical computational complexity of generating the full set of GBs is approximately $O(n)$, where n is the number of samples. This ensures that the GB generation process remains scalable to large-scale data, while maintaining high granularity adaptability and structural awareness.

IV. Shadowed Granular-Ball-based Outlier Detection Method

Traditional GB methods in outlier detection suffer from several limitations, including inadequate modeling of local uncertainty, poor handling of boundary ambiguity, and limited capacity to distinguish borderline instances. To address these issues, this paper introduces the shadowed granular-ball (SGB) framework. Built upon the conventional GB paradigm, SGB integrates fuzzy membership functions and 3WD theory to more effectively represent the internal uncertainty within each GB. First, the membership degree of a sample to a GB is defined as follows:

Definition 9. Let $U = \{x_1, x_2, \ldots, x_n\}$ be a non-empty finite set, and $G = \{gb_1, gb_2, \ldots, gb_m\}$ is a granular-ball space of U. Each $gb_i \in G(i = 1, 2, \ldots, m)$ is associated with a membership function $\mu_{gb_i} : gb_i \to [0, 1]$. The GB membership for each sample $x \in gb_i$ is formulated as follows:

$$\mu_{gb_i}(x) = \exp\left(-\frac{d(x, c_{gb_i})^2}{2\sigma^2 r_{gb_i}^2}\right) \tag{10}$$

where σ is a fuzziness coefficient that controls the rate at which the membership degree between a sample and GB decays with distance. c_{gb_i} is the center of gb_i, r_{gb_i} is the radius of gb_i, and $d(x, c_{gb_i})$ is the Euclidean distance between x and c_{gb_i}.

The fuzzy membership of a sample to a GB reflects its relative position to the GB center. When a sample is located at the center, it achieves the maximum membership value of 1, and the membership gradually decreases as the sample moves away. Then, based on the fuzzy-rough transformation theory, we defined the shadowed granular-ball (SGB) as follows:

Definition 10. Let $U = \{x_1, x_2, \ldots, x_n\}$ be a non-empty finite set, and $G = \{gb_1, gb_2, \ldots, gb_m\}$ is a granular-ball space of U. For each $gb_i \in G(i = 1, 2, \ldots, m)$, a mapping that maps GB memberships into a triplet set $\{0, [0, 1], 1\}$ can be called shadowed granular-ball, and the mapping is formulated as follows:

$$\mathbb{S}^{\alpha,\beta}_{\mu_{gb_i}}(x) = \begin{cases} 1, & \mu_{gb_i}(x) \geq \beta \\ \mu_{gb_i}(x), & \alpha < \mu_{gb_i}(x) < \beta \\ 0, & \mu_{gb_i}(x) \leq \alpha \end{cases} \tag{11}$$

Based on the threshold pair (α, β) dynamically computed from the data distribution, each GB is partitioned into three distinct regions. The detailed procedure for determining the threshold α and β of shadowed GB can be found in Section S3 of the supplementary file. To make it easier to understand, we renamed the three regions as: positive region ($\mathbb{POS}$), negative region ($\mathbb{NEG}$), and boundary region ($\mathbb{BND}$). For gb_i, its regions are defined as follows:

$$\begin{aligned} \mathbb{POS}_{gb_i} &= \{x | \mu_{gb_i}(x) \geq \beta\} \\ \mathbb{BND}_{gb_i} &= \{x | \alpha < \mu_{gb_i}(x) \leq \beta\} \\ \mathbb{NEG}_{gb_i} &= \{x | \mu_{gb_i}(x) \leq \alpha\} \end{aligned} \tag{12}$$

Based on the previously generated GBs, we first construct a fuzzy membership matrix between samples and each GB using GB membership by Equation (10). This matrix quantifies the proximity between each data object and the center of each GB, normalized by the radius to ensure scale invariance.

Subsequently, each sample x is then assigned to a decision region—positive, negative, or boundary—within the GB

gb_i based on the dynamic threshold pair (α, β), as defined in Equation (12). This division enables the model to more accurately determine the association between samples and GB by cautiously handling uncertain cases, thereby enhancing the robustness of outlier detection.

Considering that the outlier degree of an object is often more valuable than determining whether the object is an outlier in many cases, the outlier factor based on the shadowed GBs is introduced to calculate the outlier degree of the object.

Definition 11. Let $U = \{x_1, x_2, \ldots, x_n\}$ be a non-empty finite set, and $G = \{gb_1, gb_2, \ldots, gb_m\}$ is a granular-ball space of U. For each object $x \in U$, the outlier factor of x is defined as:

$$OF(x) = \sum_{i=1}^{m} \left((1 - \mathbb{S}^{\alpha,\beta}_{\mu_{gb_i}}(x)) \cdot \frac{\|x - c_i\|}{r_i} \cdot \omega_i \right) \tag{13}$$

where $\omega_i = \frac{\mathbb{E}^c_{gb_i}}{\mathbb{E}^s_{gb_i}}$ is the weight, which reflects the relative contribution of each gb_i to the outlier factor.

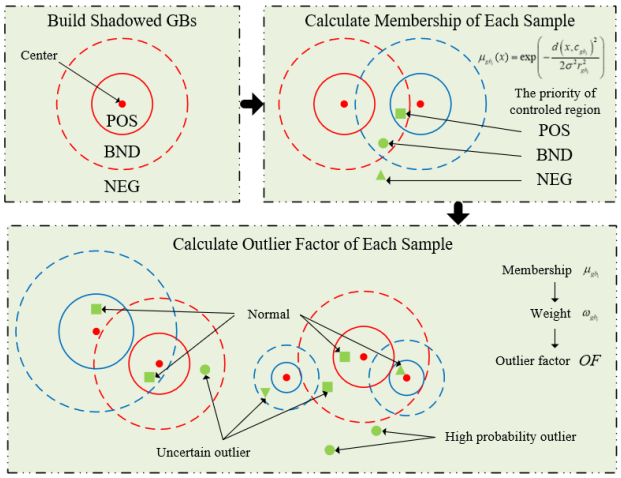

Fig. 2: Three-way outlier detection based on shadowed granular-ball

The outlier factor of an object x is computed based on the degree of abnormality of each object by comprehensively considering its fuzzy membership distribution, spatial deviation, and the quality of the granular structure. The overall process is illustrated in Fig. 2. Unlike traditional hard-assignment-based outlier scores, outlier factor leverages the three-way division mechanism and the fuzzy granularity representation introduced in 3W-SGBD to construct a soft, interpretable, and structure-aware outlier measurement.

Objects with lower memberships and larger relative distances in high-quality shadowed GBs are more likely to deviate from the data structure. Therefore, a higher outlier factor indicates a higher likelihood of being an outlier for an object. A predefined threshold ξ can be employed to delineate abnormal objects from the normal population if there is a need to distinguish certain anomalies from normal objects specifically. That is, for any $x \in U$, if $OF(x) > \xi$, x is said to be an outlier in U.

Algorithm 2: Shadowed Granular-Ball-based Outlier Detection.

Input: $IS = \langle U, C, V, f \rangle$, σ
Output: Outlier factor OF;
Initialize $OF \leftarrow \varnothing$;
Generate GB by Algorithm 1 ;
for each $x \in U$ **do**
  for each $gb_i \in G$ **do**
    Calculate membership μ_{gb_i} by Eq. 10 ;
    Calculate shadowed membership $\mathbb{S}^{\alpha,\beta}_{\mu_{gb_i}}(x)$ by Eq. 11 ;
    Assign x to $\mathbb{POS}_{gb_i}$, $\mathbb{NEG}_{gb_i}$, or $\mathbb{BND}_{gb_i}$ by Eq. 12 ;
  end
  Calculate OF by Eq. 13 ;
end
return OF.

V. Experiments

This section starts by outlining the experimental settings relevant to 3W-SGBD. Then, the performance of different methods is visually compared using ROC curves and boxplots, followed by a table summarizing the AUC values for all approaches. The effectiveness, superiority, and robustness of 3W-SGBD are next verified by data experiments and comparison analyses.

A. Experimental Settings

To validate the effectiveness of our method, we conduct several experiments on sixteen publicly available datasets. For these datasets, the number of attributes ranges from 4 to 61, the number of samples ranges from 107 to 11183, and the number of anomalies ranges from 5 to 260. The datasets used are shown in Table II.

We compare 3W-SGBD with 8 existing methods of outlier detection, including three-way neighborhood characteristic regionsnd outlier detection (3WNCROD) [41], rough membership function based algorithm (RMF) [42], boundary and distance based algorithm (BD) [43], outlier detection based on granular computing and rough set (ODGrCR) [44], sequence-based outlier detection (SEQ) [45], multi-fuzzy granules anomaly detection (MFGAD) [46] and weighted fuzzy-rough density based anomaly (WFRDA) [47].

The algorithm settings and dataset treatments refer to corresponding references. For example, the parameter values of 3WNCROD and WFRDA come from the initial settings follow the preferred parameters in the original articles. For normalization, min-max scaling is uniformly applied across all datasets. Here, some cases are generally explained. The 3WNCROD parameter λ changes in $[0.1, 2]$ with step length 0.1. The WFRDA and MFGAD parameter σ similarly changes in $[0.1, 2]$ with length 0.1. Rough set based methods RMF, BD, ODGrCR and SEQ require data discretization, and the discretization intervals are set to three bins. The fuzzy c-means (FCM) discretization method is used for datasets containingnumeric attributes.

Outlier detection algorithms typically output quantitative measures such as outlier scores, where higher values indicate greater likelihood of being anomalous. To scientifically validate and compare algorithmic performance, this study

TABLE II: Experimental datasets.

No.	Datasets	Abbr	Number of attributes	Number of samples	Number of anomalies	Anomaly ratio
1	Cardio[1]	Card	21	1831	176	9.61%
2	Cardiotocography_2and3_33_variant1[2]	Cardio	21	1688	33	1.95%
3	Diabetes_tested_positive_26_variant1[1]	Diab	8	526	26	4.94%
4	Ecoli[2]	Ecoli	8	336	9	2.68%
5	German_1_14_variant1[1]	German	20	714	14	1.96%
6	Heart270_2_16_variant1[1]	Heart	13	166	16	9.64%
7	Iris_Irisvirginica_11_variant1[1]	Iris	4	111	11	9.91%
8	Lymphography[1]	Lymp	18	148	6	4.05%
9	Mammography[1]	Mammo	6	11183	260	2.32%
10	Sick_sick_35_variant1[1]	Sick	29	3576	35	0.98%
11	Sonar_M_10_variant1[1]	Sonar	61	107	10	9.34%
12	Thyroid_disease_variant1[1]	Thyr	28	9172	74	0.80%
13	Tic_tac_toe_negative_12_variant1[1]	Tictac12	10	638	12	1.88%
14	Wbc_malignant_39_variant1[1]	Wbc	9	483	39	8.07%
15	Wdbc_M_39_variant1[1]	Wdbc	31	396	39	9.85%
16	Yeast_ERL_5_variant1[1]	Yeast	8	1141	5	0.44%

[1]https://github.com/BElloney/Outlier-detection
[2]https://github.com/Minqi824/ADBench

TABLE III: Experimental results on AUC.

Datasets	3W-SGBD	WNCROD	RMF	BD	ODGrCR	SEQ	MFGAD	WFRDA
Card	**0.942**	0.739	0.691	0.768	0.683	0.693	0.931	0.919
Cardio	**0.877**	0.850	0.674	0.741	0.710	0.604	0.769	0.847
Diab	0.950	0.954	0.908	0.874	0.921	0.870	**0.978**	**0.978**
Ecoli	**0.892**	0.554	0.848	0.323	0.853	0.842	0.587	0.634
German	0.936	0.878	0.965	0.875	0.967	0.955	0.977	**0.982**
Heart	0.970	0.980	0.969	0.936	0.967	0.971	0.989	**0.992**
Iris	**1.000**	**1.000**	0.978	0.917	0.985	0.965	0.914	**1.000**
Lymp	0.991	0.827	**0.996**	0.818	0.995	0.991	0.982	0.991
Mammo	**0.863**	0.593	0.785	0.744	0.789	0.780	0.422	0.805
Sick	0.873	0.500	**0.926**	0.500	0.911	0.886	0.523	0.816
Sonar	0.982	0.907	0.893	0.838	0.895	0.883	**0.988**	0.987
Thyr	0.658	0.500	**0.663**	0.500	0.660	0.653	0.367	0.528
Tictac12	**0.948**	0.930	0.914	0.941	0.912	0.900	0.920	0.914
Wbc	**0.997**	0.909	0.992	0.601	0.992	0.991	0.962	0.996
Wdbc	0.995	0.976	0.749	0.521	0.749	0.748	0.995	**0.999**
Yeast	**1.000**	0.599	0.995	0.992	0.988	0.996	0.995	0.993
Average	**0.930**	0.794	0.871	0.743	0.875	0.858	0.831	0.899

employs the Receiver Operating Characteristic (ROC) curve and its Area Under the Curve (AUC) as primary evaluation metrics. Additionally, Average Precision (AP) is supplemented to create a through assessment framework.

The ROC curve graphically represents the trade-off between True Positive Rate (TPR) and False Positive Rate (FPR) across varying decision thresholds, providing intuitive visualization of a model's discriminative power between outlier and normal classes. The AUC metric quantifies the overall performance through integration of the ROC curve, mathematically equivalent to the probability that a randomly chosen anomalous sample receives a higher score than a normal sample. With its value range $[0, 1]$, AUC provides a threshold-independent global evaluation, where greater values signify superior detection capability.

For extreme class imbalance scenarios (e.g., $<1\%$ anomalies in industrial equipment fault detection), we additionally introduce AP as an auxiliary metric. AP computes the area under the Precision-Recall curve, emphasizing model stability in high-recall regions. Higher AP values indicate better practical utility under low false-negative constraints. While our analysis primarily focuses on ROC-AUC, the AP metric complements the evaluation through multi-dimensional performance comparison.

B. Experimental Results

Fig. 3 shows the ROC curves of 8 methods on 16 datasets, and the orange color is the curve of 3W-SGBD. It is ob-

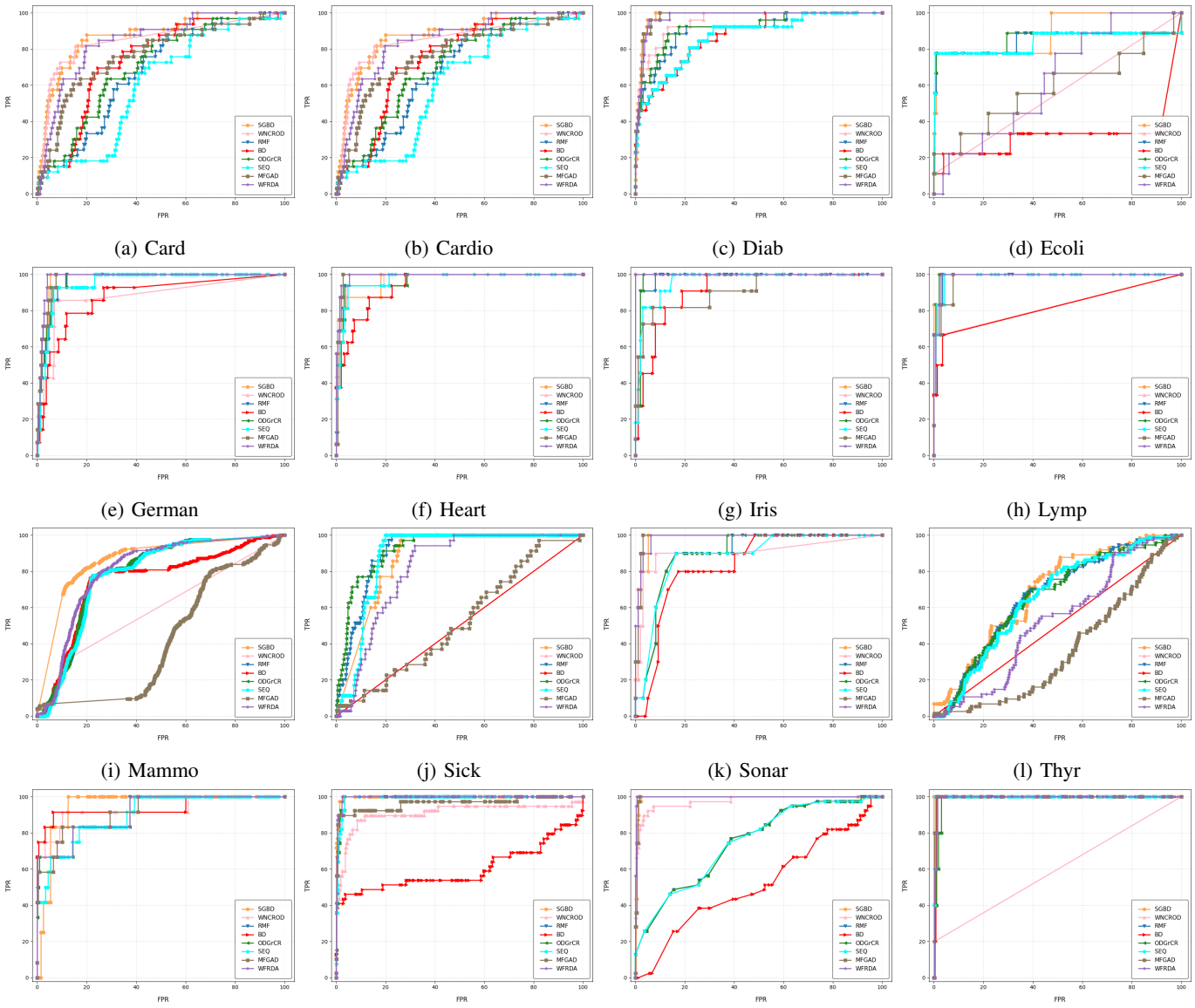

(a) Card (b) Cardio (c) Diab (d) Ecoli

(e) German (f) Heart (g) Iris (h) Lymp

(i) Mammo (j) Sick (k) Sonar (l) Thyr

(m) Tictac12 (n) Wbc (o) Wdbc (p) Yeast

Fig. 3: Experimental comparison results on ROC.

viously that 3W-SGBD outperforms the other methods on most datasets. Next, we compare the AUC values of the 8 methods on different datasets. The AUC values of different methods are shown in Table III, where the bold labels optimal values on datasets. Among them, 3W-SGBD performs the best on most datasets, e.g., Card, Cardio, Iris, Wbc, Yeast, etc. The average AUC values of 3W-SGBD is 0.930, which is significantly better than other methods. Moreover, the AP results are recorded in Table IV. The average AP values of 3W-SGBD is 0.593, and exceeds other comparison algorithms.

As illustrated in Fig. 4, the AUC boxplots for various methods across all datasets are presented. These boxplots serve as valuable tools for visualizing the distribution of AUC values for different methods when applied to diverse datasets, thereby offering insights into the stability of these methods. Fig. 4 reveals that 3W-SGBD exhibits a notably more compact and upward form. This observation implies that 3W-SGBD demonstrates superior performance and showcases commendable stability, underlining its efficacy as a robust outlier detection method.

The running times of all comparison experiments are reported in Table V. From Table V, 3W-SGBD has a moderate running time, and its temporal cost is also less than that of MFGAD and WFRDA. Thus, it is feasible and effective in practical applications.

C. Statistical Test Analysis

Friedman test and Nemenyi test are adopted here to evaluate the statistical significance [48], [49]. First, the Friedman test is used to determine whether different methods achieve the same performance. After that, the Nemenyi test further discriminates the methods, and the Nemenyi test figure visualizes the differences between the methods.

TABLE IV: Experimental results on AP.

Datasets	3W-SGBD	3WNCROD	RMF	BD	ODGrCR	SEQ	MFGAD	WFRDA
Card	**0.637**	0.294	0.365	0.375	0.351	0.355	0.625	0.526
Cardio	**0.139**	**0.139**	0.047	0.054	0.046	0.040	0.080	0.089
Diab	0.675	0.609	0.559	0.493	0.594	0.484	0.688	**0.713**
Ecoli	**0.655**	0.135	0.612	0.147	0.623	0.629	0.255	0.049
German	0.440	0.229	0.351	0.197	0.358	0.264	**0.452**	0.438
Heart	0.855	0.884	0.787	0.694	0760	0.809	0.838	**0.933**
Iris	**1.000**	**1.000**	0.772	0.558	0.836	0.747	0.719	**1.000**
Lymp	**0.944**	0.680	0.821	0.521	0.917	0.869	0.818	0.871
Mammo	**0.116**	0.055	0.054	0.053	0.055	0.052	0.061	0.066
Sick	0.039	0.010	0.086	0.010	**0.121**	0.042	0.014	0.026
Sonar	0.823	0.685	0.423	0.276	0.423	0.428	0.866	**0.891**
Thyr	**0.080**	0.008	0.012	0.008	0.012	0.012	0.007	0.008
Tictac12	0.177	0.720	0.690	**0.772**	0.595	0.490	0.577	0.671
Wbc	**0.966**	0.692	0.884	0.460	0.891	0.865	0.855	0.952
Wdbc	0.900	0.889	0.328	0.116	0.328	0.324	0.934	**0.985**
Yeast	**1.000**	0.204	0.408	0.243	0.299	0.464	0.348	0.323
Average	**0.593**	0.443	0.445	0.315	0.445	0.425	0.515	0.533

TABLE V: Running times of different methods (unit: seconds).

Datasets	3W-SGBD	3WNCROD	RMF	BD	ODGrCR	SEQ	MFGAD	WFRDA
Card	8.479	357.323	1563.155	12.219	9260.842	13.928	30.316	50.337
Cardio	9.477	279.781	1157.764	9.418	1768.140	11.284	22.981	48.552
Diab	0.790	18.535	9.429	0.622	30.659	0.268	0.479	2.089
Ecoli	0.426	0.236	1.140	0.211	1.965	0.098	0.116	0.692
German	1.360	3.486	97.965	2.577	217.391	2.000	4.551	7.475
Heart	0.198	0.277	0.652	0.221	2.273	0.072	0.130	0.402
Iris	0.123	0.029	0.046	0.029	0.105	0.008	0.010	0.037
Lymp	0.198	0.155	0.556	0.187	0.457	0.060	0.102	0.294
Mammo	135.636	3133.778	53160.775	140.248	156037.609	217.356	398.020	587.044
Sick	26.055	74.999	20038.002	74.149	13659.638	123.982	227.132	280.524
Sonar	0.182	0.592	2.089	0.530	185.845	0.099	0.466	0.524
Thyr	138.192	3133.000	51605.877	124.408	80887.820	193.671	302.880	507.706
Tictac12	1.067	1.252	16.040	0.666	2.049	0.746	0.733	3.105
Wbc	0.665	0.720	8.783	0.560	4.097	0.492	0.485	1.831
Wdbc	0.819	1.543	31.250	1.359	1542.817	0.770	3.437	3.678
Yeast	2.623	2.975	90.727	1.683	68.319	1.624	2.251	7.614
Average	20.393	438.043	7986.177	23.084	16479.377	35.404	62.131	93.619

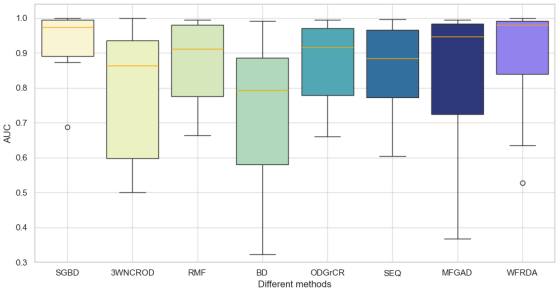

Fig. 4: The AUC boxplots for each method across 16 datasets.

To compare the AUC values of different algorithms across multiple datasets, the AUC values for each dataset are first arranged in ascending order and assigned corresponding ranks (e.g., 1st, 2nd, ...). In cases where multiple algorithms yield identical AUC values on a dataset, the tied algorithms are assigned the arithmetic mean of their ranks. Subsequently, the Friedman test is employed to statistically assess the overall performance differences among M algorithms evaluated on N datasets. According to the method described in [48], the Friedman test statistic τ_F is computed and follows an F-distribution with degrees of freedom $(M-1)$ and $(M-1)(N-1)$. A significant test result, i.e., rejection of the null hypothesis that all algorithms perform equivalently, indicates that statistically significant differences exist among at least

some of the algorithms.

To further delineate the specific differences between the algorithms, the Nemenyi test is adopted. This test computes the Critical Difference (CD) based on the average ranks of the algorithms. The criterion is that if the difference between the average ranks of any two algorithms exceeds CD_ζ, their performance difference is considered statistically significant. The CD is computed as follows [49]:

$$CD_\zeta = q_\zeta \sqrt{\frac{M(M+1)}{6N}} \tag{14}$$

where q_ζ is the critical value from the Tukey distribution at the significance level ζ. The Nemenyi test results are typically presented graphically, providing an intuitive visualization of the significant differences among the algorithms and furnishing robust support for subsequent detailed comparative analysis.

As seen in Table III, 8 methods and 16 datasets are utilized in our experiment. The F distributions with degrees of freedom of 7 and 105 can be obtained. According to the Friedman test, when $\zeta = 0.05$, the value of $\tau_F = 9.3902$ is greater than the critical value 2.098. Therefore, the null hypothesis that "all the methods have the same performance" does not hold. In other words, the methods are significantly different, and a post-hoc test is needed to further distinguish between them.

According to the Nemenyi test, when the significance level $\zeta = 0.05$, the corresponding critical distance $CD_{0.05} = 2.6248$. By plotting the average ordinal value of all methods and the line segment of CD length on a single axis, the Nemenyi test figure is shown in Fig. 5. When there is a red horizontal line segment CD covering between some methods in Fig. 5, it is assumed that there are no statistical differences between these methods. It can be seen that there is no horizontal line segment coverage between 3W-SGBD, MFGAD, ODGrCR, BD, SEQ, 3WNCROD, RMF, and it is considered that there are significant statistical differences between 3W-SGBD and these methods.

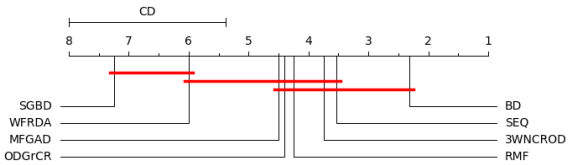

Fig. 5: Nemenyi test figure on AUC.

D. Effect of attribute noise on AUC values

We follow the method described in [47] to evaluate the impact of attribute noise on the performance of 3W-SGBD. Attribute noise is introduced through two steps: first, we add an error of $t \cdot 100\%$ to each attribute; then, we randomly replace the values of $[t \cdot n]$ objects in the corresponding attribute with random values. For numerical attributes, replacement values are sampled uniformly within the attribute's original range; for nominal attributes, random categories are selected from the attribute domain.

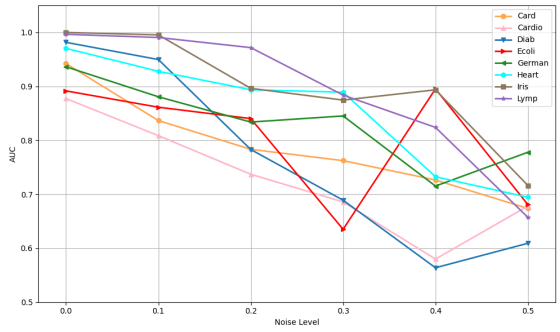

Fig. 6: The variation curves of AUC with attribute noise level on datasets 1-8.

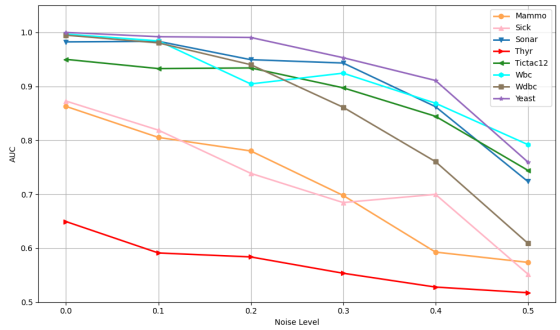

Fig. 7: The variation curves of AUC with attribute noise level on datasets 9-16.

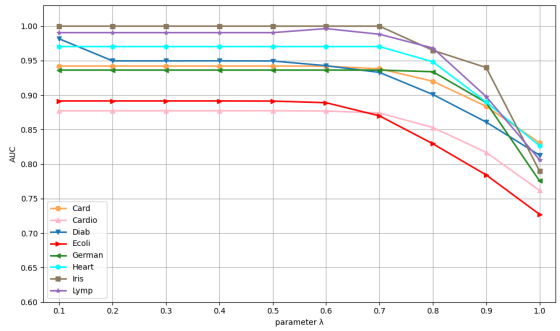

Fig. 8: The variation curves of AUC with parameter λ on datasets 1-8.

The results illustrate the effect of attribute noise on the AUC values are presented in Fig. 6 and Fig. 7. As the noise level increases, the AUC performance exhibits certain fluctuations across different datasets. However, the degree of fluctuation remains relatively limited. In particular, the 3W-GBD algorithm maintains stable performance on datasets such as Card, Ecoli, Iris, Thyr and Yeast, even under higher noise levels. These observations indicate that 3W-SGBD is robust to attribute noise, demonstrating strong resilience in maintaining detection capability across varying noise intensities.

E. Ablation study

To further validate the necessity and effectiveness of the proposed granular-ball generation designs, we conducted compre-

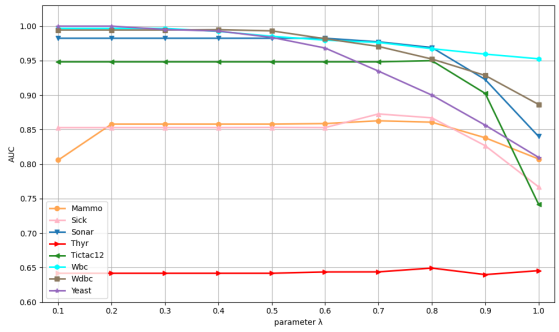

Fig. 9: The variation curves of AUC with parameter λ on datasets 9-16.

hensive ablation experiments on the same benchmark datasets used in the main experiments. Specifically, three variants of our framework were compared. The first is the full model, which includes both the entropy-based granular-ball quality measurement and the loss-controlled partitioning strategy. The second variant, without loss control, removes the loss-guided mechanism and partitions granular-balls solely through conventional clustering. The third variant, without the three-way decision, replaces the proposed three-way decision-based anomaly scoring with a simple distance-based scoring scheme.

The results in Fig. 10 show that the full model consistently achieves the best performance across most benchmark datasets. In particular, removing the loss-control mechanism leads to a significant decrease in AUC, highlighting the importance of entropy-guided granular-ball generation. Similarly, excluding the three-way decision mechanism also causes a moderate performance drop. For completeness, the detailed numerical results are provided in Section S4 of the supplementary material. These ablation results collectively validate the necessity and effectiveness of our proposed granular-ball generation and decision-making strategy.

F. Parameter sensitivity analysis

To further validate the stability and robustness of 3W-SGBD, this section conducts a systematic parameter sensitivity analysis with respect to the key parameter λ. Fig. 8 and Fig. 9 illustrate the AUC curves obtained on 16 public benchmark datasets under varying values of λ. This figure sets the adjustable range of λ to [0, 1] and the step size to 0.1.

The results show that 3W-SGBD exhibits excellent robustness across most datasets. As λ changes, the AUC values remain relatively stable over a wide range, indicating that the performance of 3W-SGBD is not highly sensitive to the selection of λ. However, on a few datasets, when λ approaches 1.0, the AUC values experience a noticeable decline. This is because a larger λ leads to excessively coarse GBs, ignoring subtle local outlier structures and reducing detection accuracy. Conversely, when λ is set too small, the resulting GBs become overly fine-grained and are more susceptible to noise interference, which may also negatively impact performance.

The reasons that 3W-SGBD can improve outlier detection performance can be summarized as follows: SGB introduces the concept of shadowed GBs to represent data regions with inherent uncertainty. By constructing coarse-to-fine granules adaptively, SGB can effectively reduce the influence of noisy data and preserve the essential structures of the dataset. Building upon SGB, the 3W-SGBD model integrates three-way decision theory, allowing for a flexible assignment of instances into positive, negative, and boundary regions based on fuzzy membership values. This hierarchical decision mechanism enables 3W-SGBD to handle uncertainty and borderline samples more effectively. Moreover, 3W-SGBD uses a composite loss function that combines coverage entropy and specificity entropy to guide the formation and splitting of GBs. This dual-entropy-driven mechanism ensures that each GB maintains both sufficient information coverage and high discriminatory power, thereby improving the overall outlier detection precision. Instead of relying on a single granularity, 3W-SGBD leverages multiple GBs of varying sizes, capturing data characteristics from multiple levels of granularity and enhancing robustness against local noise perturbations. During the outlier scoring phase, 3W-SGBD further incorporates adaptive weighting based on the GB's coverage and specificity. Samples that fall into important regions are evaluated according to their relative distances and the weights of the associated GBs. In addition, potential noisy GBs are detected and specially treated with adjusted weights, enhancing the model's sensitivity to subtle outliers. In summary, 3W-SGBD's ability to dynamically adapt granularity, mitigate uncertainty through three-way decision-making, and jointly optimize coverage and specificity through entropy-based learning allows it to achieve superior and stable outlier detection performance across various datasets.

To further validate the generalizability of the proposed framework, additional experiments on image anomaly detection have been conducted, and the detailed results are provided in Section S5 of the supplementary material.

VI. Conclusion

In this study, we propose an effective outlier detection method named three-way outlier detection based on shadowed granular-ball (3W-SGBD), which integrates GBC with an adaptive hierarchical density-based clustering strategy to enhance the detection of anomalies. By leveraging the compound loss function composed of coverage entropy and specificity entropy, our proposed method dynamically guides the generation and division of GBs, effectively capturing the structural and uncertainty characteristics of the data distribution. Furthermore, the introduction of a three-way decision mechanism enables 3W-SGBD to provide a finer-grained assessment of the outlier degree, leading to more robust and interpretable detection results. Extensive experiments conducted on a variety of public datasets demonstrate that 3W-SGBD consistently outperforms most existing methods, achieving higher detection accuracy, strong robustness to noise, and stable performance across different types of datasets. The experimental analysis also highlights the advantages of the multi-granularity and dual-entropy-driven GB generation in addressing challenges such as overlapping clusters and local density variations.

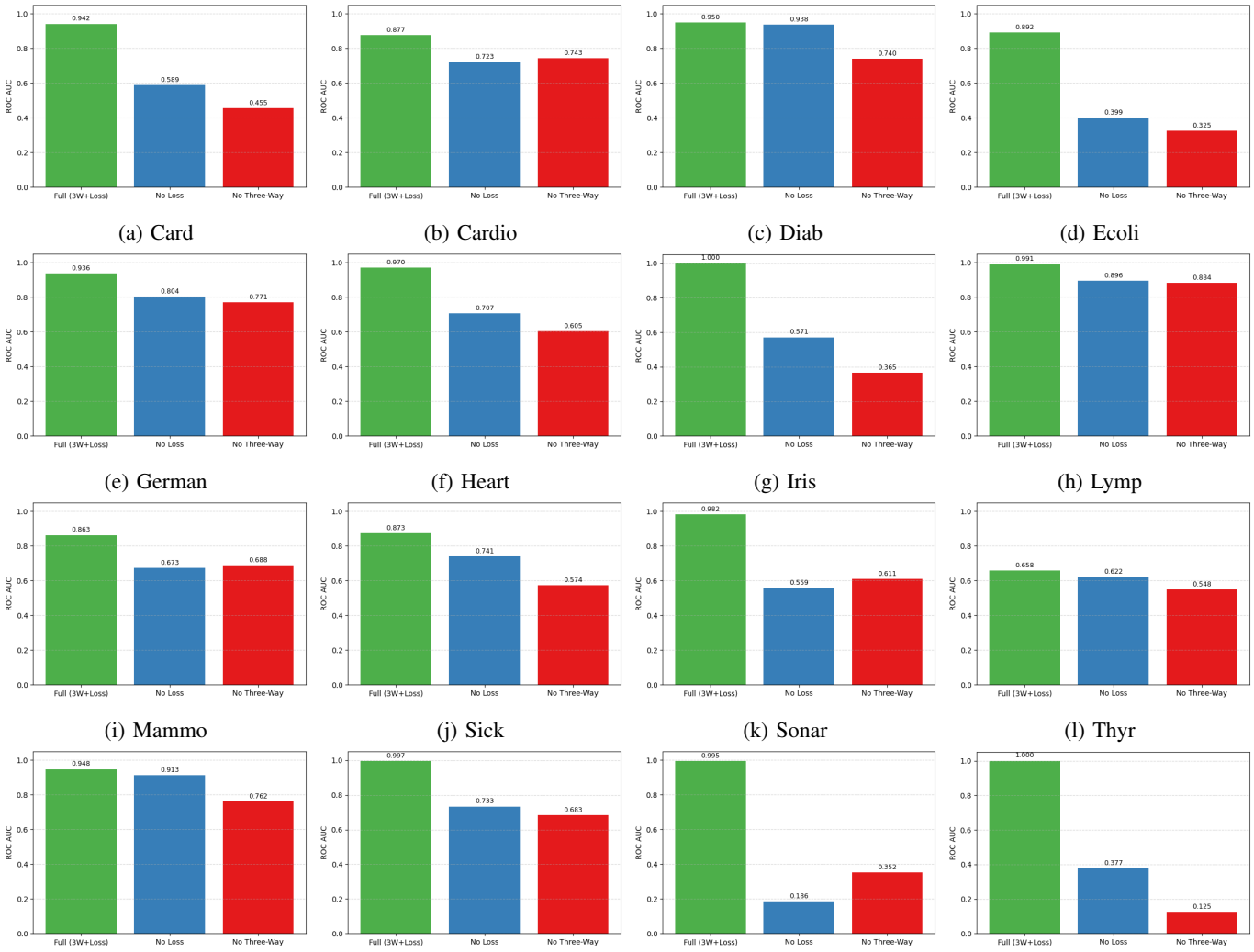

(a) Card (b) Cardio (c) Diab (d) Ecoli

(e) German (f) Heart (g) Iris (h) Lymp

(i) Mammo (j) Sick (k) Sonar (l) Thyr

(m) Tictac12 (n) Wbc (o) Wdbc (p) Yeast

Fig. 10: Ablation study results.

Despite its promising performance, certain limitations remain. In particular, the granular-ball-splitting process relies on HDBSCAN, which may encounter difficulties when the dataset exhibits subtle density variations, potentially affecting the precision of boundary delineation. Additionally, the selection of thresholds α and β in the three-way decision framework requires careful adjustment for different datasets, which can increase the complexity of practical deployment. Future work will focus on designing adaptive threshold optimization strategies and exploring alternative GB generation methods to further enhance the flexibility and generalization capability of 3W-SGBD. Moreover, addressing the challenges posed by high-dimensional data and developing tailored techniques for handling categorical or mixed-type attributes are also promising directions for future research.

ACKNOWLEDGMENT

This work was supported by the National Science Foundation of China (Grant number 62466063, 62221005, 62302030, 62176070), the Guizhou Provincial Department of Education Colleges and Universities Science and Technology Innovation Team (QJJ[2023]084), the New Chongqing Youth Innovation Talent Projectand under Grant CSTB2024NSCQ-QCXMX0035.

REFERENCES

[1] D. M. Hawkins, *Identification of outliers*. Springer, 1980, vol. 11.
[2] X. Wang, Z. Liu, J. Liu, and J. Liu, "Fraud detection on multi-relation graphs via imbalanced and interactive learning," *Information Sciences*, vol. 642, p. 119153, 2023.
[3] W. Xiaolan, M. M. Ahmed, M. N. Husen, Z. Qian, and S. B. Belhaouari, "Evolving anomaly detection for network streaming data," *Information Sciences*, vol. 608, pp. 757–777, 2022.
[4] K. Yang, W. Chen, J. Bi, M. Wang, and F. Luo, "Multi-view broad learning system for electricity theft detection," *Applied Energy*, vol. 352, p. 121914, 2023.
[5] P. J. Rousseeuw and A. M. Leroy, *Robust regression and outlier detection*. John wiley & sons, 2003.
[6] E. M. Knorr, R. T. Ng, and V. Tucakov, "Distance-based outliers: algorithms and applications," *The VLDB Journal*, vol. 8, no. 3, pp. 237–253, 2000.
[7] B. Tang and H. He, "A local density-based approach for outlier detection," *Neurocomputing*, vol. 241, pp. 171–180, 2017.
[8] Z. He, X. Xu, and S. Deng, "Discovering cluster-based local outliers," *Pattern recognition letters*, vol. 24, no. 9-10, pp. 1641–1650, 2003.

[9] A. Albanese, S. K. Pal, and A. Petrosino, "Rough sets, kernel set, and spatiotemporal outlier detection," *IEEE Transactions on knowledge and data engineering*, vol. 26, no. 1, pp. 194–207, 2012.

[10] A. Degirmenci and O. Karal, "Efficient density and cluster based incremental outlier detection in data streams," *Information Sciences*, vol. 607, pp. 901–920, 2022.

[11] Z. Yuan, H. Chen, T. Li, B. Sang, and S. Wang, "Outlier detection based on fuzzy rough granules in mixed attribute data," *IEEE Transactions on Cybernetics*, vol. 52, no. 8, pp. 8399–8412, 2021.

[12] M. M. Breunig, H.-P. Kriegel, R. T. Ng, and J. Sander, "Lof: identifying density-based local outliers," in *Proceedings of the 2000 ACM SIGMOD international conference on Management of data*, 2000, pp. 93–104.

[13] K. Feasel, "Connectivity-based outlier factor (cof)," in *Finding Ghosts in Your Data: Anomaly Detection Techniques with Examples in Python*. Springer, 2022, pp. 185–201.

[14] W. Jin, A. K. Tung, J. Han, and W. Wang, "Ranking outliers using symmetric neighborhood relationship," in *Advances in Knowledge Discovery and Data Mining: 10th Pacific-Asia Conference, PAKDD 2006, Singapore, April 9-12, 2006. Proceedings 10*. Springer, 2006, pp. 577–593.

[15] R. J. Campello, D. Moulavi, and J. Sander, "Density-based clustering based on hierarchical density estimates," in *Pacific-Asia conference on knowledge discovery and data mining*. Springer, 2013, pp. 160–172.

[16] J. Qin, L. Martínez, W. Pedrycz, X. Ma, and Y. Liang, "An overview of granular computing in decision-making: Extensions, applications, and challenges," *Information Fusion*, vol. 98, p. 101833, 2023.

[17] W. Ding, W. Pedrycz, I. Triguero, Z. Cao, and C.-T. Lin, "Multigranulation supertrust model for attribute reduction," *IEEE Transactions on Fuzzy Systems*, vol. 29, no. 6, pp. 1395–1408, 2020.

[18] S. Xia, G. Wang, X. Gao, and X. Lian, "Granular-ball computing: an efficient, robust, and interpretable adaptive multi-granularity representation and computation method," *arXiv e-prints*, pp. arXiv–2304, 2023.

[19] S. Xia, X. Dai, G. Wang, X. Gao, and E. Giem, "An efficient and adaptive granular-ball generation method in classification problem," *IEEE Transactions on Neural Networks and Learning Systems*, vol. 35, no. 4, pp. 5319–5331, 2022.

[20] W. Qian, W. Ruan, Y. Li, and J. Huang, "Granular ball-based label enhancement for dimensionality reduction in multi-label data," *Applied Intelligence*, vol. 53, no. 20, pp. 24 008–24 033, 2023.

[21] J. Yang, Z. Liu, G. Wang, Q. Zhang, S. Xia, D. Wu, and Y. Liu, "Constructing three-way decision with fuzzy granular-ball rough sets based on uncertainty invariance," *IEEE Transactions on Fuzzy Systems*, 2025.

[22] J. Xie, X. Xiang, S. Xia, L. Jiang, G. Wang, and X. Gao, "Mgnr: A multi-granularity neighbor relationship and its application in knn classification and clustering methods," *IEEE Transactions on Pattern Analysis and Machine Intelligence*, 2024.

[23] H. Bai, F. Shen, W. Kong, and J. Feng, "Granular-ball clustering based neighbourhood outliers detection method," in *2023 6th International Conference on Electronics Technology (ICET)*. IEEE, 2023, pp. 1306–1312.

[24] X. Su, Z. Yuan, B. Chen, D. Peng, H. Chen, and Y. Chen, "Detecting anomalies with granular-ball fuzzy rough sets," *Information Sciences*, vol. 678, p. 121016, 2024.

[25] S. Cheng, X. Su, B. Chen, H. Chen, D. Peng, and Z. Yuan, "Gbmod: A granular-ball mean-shift outlier detector," *Pattern Recognition*, vol. 159, p. 111115, 2025.

[26] Y. Yao, "Three-way decision and granular computing," *International Journal of Approximate Reasoning*, vol. 103, pp. 107–123, 2018.

[27] Y. Yao, "Three-way granular computing, rough sets, and formal concept analysis," *International Journal of Approximate Reasoning*, vol. 116, pp. 106–125, 2020.

[28] D. Dubois and H. Prade, "Rough fuzzy sets and fuzzy rough sets," *International Journal of General System*, vol. 17, no. 2-3, pp. 191–209, 1990.

[29] W. Pedrycz, "Shadowed sets: representing and processing fuzzy sets," *IEEE Transactions on Systems, Man, and Cybernetics, Part B (Cybernetics)*, vol. 28, no. 1, pp. 103–109, 1998.

[30] L. A. Zadeh, "Fuzzy sets," *Information and control*, vol. 8, no. 3, pp. 338–353, 1965.

[31] W. Pedrycz and G. Vukovich, "Granular computing with shadowed sets," *International Journal of Intelligent Systems*, vol. 17, no. 2, pp. 173–197, 2002.

[32] Q. Zhang, Y. Xiao, and G. Wang, "A new method for measuring fuzziness of vague set (or intuitionistic fuzzy set)," *Journal of Intelligent & Fuzzy Systems*, vol. 25, no. 2, pp. 505–515, 2013.

[33] Y. Yao, "Three-way decisions with probabilistic rough sets," *Information sciences*, vol. 180, no. 3, pp. 341–353, 2010.

[34] Z. Jia, Z. Zhang, and W. Pedrycz, "Generation of granular-balls for clustering based on the principle of justifiable granularity," *IEEE Transactions on Cybernetics*, vol. 55, no. 4, pp. 1687–1700, 2025.

[35] D. Cheng, S. Liu, S. Xia, and G. Wang, "Granular-ball computing-based manifold clustering algorithms for ultra-scalable data," *Expert Systems with Applications*, vol. 247, p. 123313, 2024.

[36] D. Cheng, C. Zhang, Y. Li, S. Xia, G. Wang, J. Huang, S. Zhang, and J. Xie, "Gb-dbscan: a fast granular-ball based dbscan clustering algorithm," *Information Sciences*, vol. 674, p. 120731, 2024.

[37] Q. Haenn, B. Chardin, and M. Baron, "Clustering under radius constraints using minimum dominating sets," in *International Symposium on Methodologies for Intelligent Systems*. Springer, 2024, pp. 14–23.

[38] Y. Ni, J. Qian, E. Chen, S. Yan, and J. Ye, "Gbk-dpc: Density peak clustering based on granular ball with k-nearest neighbor," *Pattern Recognition*, p. 112243, 2025.

[39] W. Pedrycz and W. Homenda, "Building the fundamentals of granular computing: A principle of justifiable granularity," *Applied Soft Computing*, vol. 13, no. 10, pp. 4209–4218, 2013.

[40] W. Pedrycz and X. Wang, "Designing fuzzy sets with the use of the parametric principle of justifiable granularity," *IEEE Transactions on Fuzzy Systems*, vol. 24, no. 2, pp. 489–496, 2015.

[41] X. Zhang, Z. Yuan, and D. Miao, "Outlier detection using three-way neighborhood characteristic regions and corresponding fusion measurement," *IEEE Transactions on Knowledge and Data Engineering*, vol. 36, no. 5, pp. 2082–2095, 2023.

[42] F. Jiang, Y. Sui, and C. Cao, "A rough set approach to outlier detection," *International Journal of General Systems*, vol. 37, no. 5, pp. 519–536, 2008.

[43] F. Jiang, Y. Sui, and C. Cao, "A hybrid approach to outlier detection based on boundary region," *Pattern recognition letters*, vol. 32, no. 14, pp. 1860–1870, 2011.

[44] F. Jiang and Y.-M. Chen, "Outlier detection based on granular computing and rough set theory," *Applied intelligence*, vol. 42, pp. 303–322, 2015.

[45] F. Jiang, Y. Sui, and C. Cao, "Some issues about outlier detection in rough set theory," *Expert Systems with Applications*, vol. 36, no. 3, pp. 4680–4687, 2009.

[46] Z. Yuan, H. Chen, C. Luo, and D. Peng, "Mfgad: Multi-fuzzy granules anomaly detection," *Information Fusion*, vol. 95, pp. 17–25, 2023.

[47] Z. Yuan, B. Chen, J. Liu, H. Chen, D. Peng, and P. Li, "Anomaly detection based on weighted fuzzy-rough density," *Applied Soft Computing*, vol. 134, p. 109995, 2023.

[48] M. Friedman, "A comparison of alternative tests of significance for the problem of m rankings," *The annals of mathematical statistics*, vol. 11, no. 1, pp. 86–92, 1940.

[49] J. Demšar, "Statistical comparisons of classifiers over multiple data sets," *Journal of Machine learning research*, vol. 7, no. Jan, pp. 1–30, 2006.